High-Level Computational Studies of Nonidentity Proton Transfer Reactions: Variations in Their Gas Phase Potential Energy Surfaces

Scott Gronert* and Cliff Kimura

Department of Chemistry and Biochemistry, San Francisco State University, San Francisco, California 94132

Received: July 21, 2003; In Final Form: August 22, 2003

High-level calculations (G2+) have been used to characterize the gas phase potential energy surfaces of the nonidentity proton transfer reactions of a series of simple anions (H^-, CH_3^-, NH_2^-, OH^-, F^-, SiH_3^-, PH_2^-, SH^-, Cl^-, HCC^-, and NC^-) with their conjugate acids. Only the combinations that give reactions that are exothermic by less than 20 kcal/mol were considered. The surfaces for the nonidentity reactions appear to be hybridizations of those of the corresponding identity reactions, and a simple averaging approach provides a reasonable representation of the nonidentity surface. Measures based on the geometry or electron density indicate that the position of the transition state ("early" or "late") is better correlated with the properties of the proton donor/acceptor than the exothermicity of the proton transfer process in these systems.

Introduction

Proton transfer is one of the most fundamental processes in chemistry and it is a key component in many organic and biochemical transformations.[1−9] It is no surprise that proton transfer has been the subject of innumerable experimental and computational studies over the past century. In an earlier paper, we reported high-level calculations on the gas phase, identity proton transfer reactions between simple hydrides ($AH + A^- \rightarrow A^- + AH$, A = CH_3, NH_2, OH, F, SiH_3, PH_2, SH, Cl).[10] In that work, we found a strong correlation between the electronegativity of the central atom and the barrier to the proton transfer. We interpreted this result in terms of a model where the transition state was dominated by an ionic resonance form where the transferring proton and bases carried full charges (Scheme 1). Clearly, this resonance form would be most stable when A is highly electronegative. Since then, several theoretical studies related to gas phase identity proton transfer reactions have appeared and, in general, have provided added support for this type of charge distribution in the transition state.[11−21]

In the present work, we extend these studies to consider nonidentity proton transfer reactions involving the same species from the previous study as well as a few others ($A_1H + A_2^- \rightarrow A_1^- + A_2H$, $A_1 \neq A_2$). Here, we wish to examine how the nature of the reaction partners affects the shape of the reaction surface. In gas phase proton transfer reactions, two general types of potential energy surfaces are possible: (a) double-well potential with a barrier or (b) single-well potential. These are illustrated in Figure 1. Because there is always an attraction between an anion and a molecule in the gas phase, the initial portion of the potential energy surface must be stabilizing and leads to an ion/molecule complex. If the proton transfer process has an energy demand, a transition state will appear on the surface, separating a pair of ion/molecule complexes (reactant and product complexes). This leads to a double-well surface (Figure 1a). On the other hand, the ion/molecule complex that is formed can have a very strong hydrogen bonding interaction leading to a situation where the proton is shared by the partners. In this case, there is no barrier to proton transfer and a single-well potential results (Figure 1b). In our earlier work, both types of surfaces were found. Here, we are especially interested in investigating the potential energy surfaces of systems where the reaction partners gave different types of surfaces in their identity reactions (i.e., A_1H gave a double-well and A_2H gave a single-well).

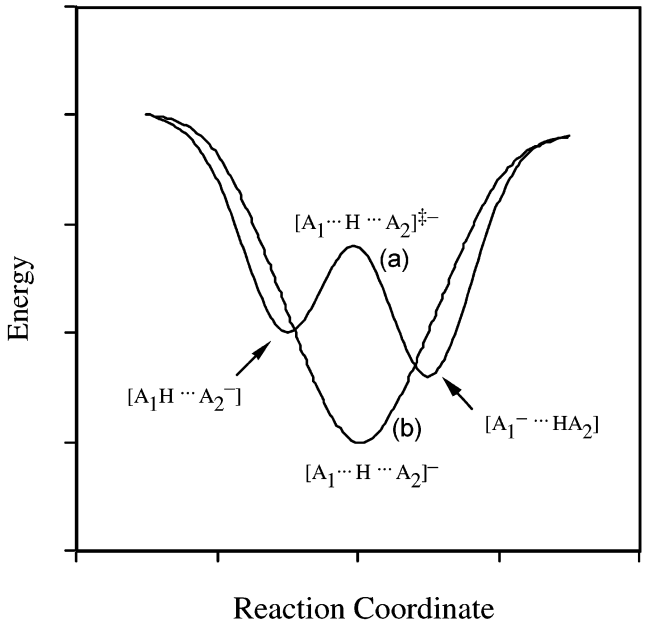

Figure 1. Generic plots of (a) double and (b) single-well potential energy surfaces for gas phase reactions.

SCHEME 1

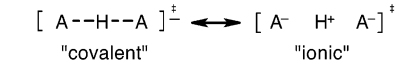

Calculations

Energies. Ab initio calculations were completed using the Gaussian92[22] quantum mechanical package. Geometries were optimized using 6-31G(d,p) (neutrals) or 6-31+G(d,p) (anions) basis sets at the Hartree−Fock and MP2 levels. At the Hartree−Fock level, the character of all minima and transition states was confirmed with analytical second derivatives. Relative energies are corrected for zero-point vibrations (Hartree−Fock values

10.1021/jp036131e CCC: $25.00
Published on Web 09/27/2003

scaled by 0.9135).[23] The basis sets for the calculations of the isolated conjugate bases were augmented with a set a hydrogen functions placed at the approximate position of the missing proton—the functions are centered at a point in space that best matches the X−H bond lengths and angles found in the parent hydride. In our earlier study,[10] we found that this was an efficient approach to improving the accuracy of the calculations. Although counterpoise approaches of this type have been criticized, acidities represent a special case because the acid and conjugate base contain the same number of electrons; therefore, ghost functions are necessary to keep a constant (basis function)/(electron) ratio. For H^-, a modified basis set was required. The standard 6-31++G(d,p) basis was tested, but its diffuse function is not adequate for hydride. To alleviate this problem, a more diffuse s-function (exp = 0.010) was added to the basis set for H^-. At the highest level of theory, the reaction energies are converted to 298 K by a calculation of integrated heat capacities. Standard methods employing the ab initio vibrational frequencies were used for these calculations.[24]

For accurate energies, a modified G2 approach[25] was taken (G2+).[10] Using the MP2/6-31+G(d,p) geometries, single point calculations were completed at the MP4/6-311+G(2df,p), QCISD(T)/6-311+G(d,p), and MP2/6-311+G(3df,2p) levels. Using the MP4/6-311+G(2df,p) level as a starting point, a correction is made for higher level correlation (ΔE(QCI)),

$$\Delta E(\mathrm{QCI}) = \{\mathrm{QCISD(T)/6\text{-}311+G(d,p)}\} - \{\mathrm{MP4/6\text{-}311+G(d,p)}\}$$

and basis set enhancement (ΔE(3df,2p))

$$\Delta E(\mathrm{3df,2p}) = \{\mathrm{MP2/6\text{-}311+G(3df,2p)}\} - \{\mathrm{MP2/6\text{-}311+G(2df,p)}\}$$

The energies are also corrected for zero point vibrations (ΔE(ZPE)). In addition, an empirical, higher-level correlation (Δ(HLC)) correction based on the number of paired and unpaired electrons is made. This term cancels out in all of the reactions in this study because none of them involve a change in the number of paired electrons.

$$\Delta E(\mathrm{HLC}) = -0.00481\ (\text{no. of } \beta \text{ valence electrons}) - 0.00019\ (\text{no. of } \alpha \text{ valence electrons})$$

in hartrees ($\alpha \geq \beta$)

The G2+ energy is the sum of these corrections:

$$\mathrm{G2+} = \mathrm{MP4/6\text{-}311+G(2df,p)} + \Delta E(\mathrm{QCI}) + \Delta E(\mathrm{3df,2p}) + \mathrm{ZPE} + \Delta E(\mathrm{HLC})$$

As outlined above, a counterpoise approach was used in calculating proton affinities and reaction energies. Moreover, the augmented 6-311++G basis set was used for H^-.

Calculations were completed on a cluster of Hewlett-Packard 720 workstations at the San Francisco State University Computational Chemistry and Visualization Center or a Hewlett-Packard 735 workstation.

Electron Density Analysis. Electron density analysis was completed using Bader's approach with a modified version of the PROAIM program.[26] Electron density analysis was completed at the MP2/6-31+G(d,p) level (diffuse functions were omitted for neutral compounds). The application of Bader's approach has been discussed in detail elsewhere,[26] so only a brief description is provided here. The n_x values represent the integrated densities within the zero-flux surfaces surrounding atom X in the molecular wave function. They provide rigorously defined, physically meaningful measures of the charges on each of the atoms. Previous work has shown that this approach is far superior to conventional Mulliken population analysis.[27] The ρ value is the density at the critical point of a bond where the critical point is defined as the density minimum along the bond path connecting the two atoms. In earlier work, it has been shown that relative ρ values provide a reasonable measure of the bond order.[28,29] However, the absolute value of ρ is dependent on the size of the atoms and comparisons between different bonding partners is difficult.

TABLE 1: G2+ Proton Affinities[a]

	proton affinity	
structure	computed	expt[b]
H^-	401.1	400.4 ± 0.1
CH_3^-	416.9	416.7 ± 0.7
NH_2^-	404.0	404.3 ± 0.3
OH^-	390.5	390.7 ± 0.1
F^-	371.0	371.6 ± 0.2
SiH_3^-	373.1	372.8 ± 0.8
PH_2^-	368.0	370.8 ± 2.1
SH^-	350.7	350.7 ± 0.9
Cl^-	332.6	333.4 ± 0.1
$HC{\equiv}C^-$	376.8	378.0 ± 0.6
$N{\equiv}C^-$	350.7	351.1 ± 2.1

[a] Energies in kcal/mol. See text for details on G2+. [b] See ref 33. When more than one value was given in the reference, the one with the smallest uncertainty was generally used.

Results and Discussion

1. Proton Affinities. In our earlier study, the G2+ proton affinities of the conjugate bases of the first and second-row nonmetal hydrides were reported.[10] Those values are given in Table 1 along with values for the three new bases in this study, H^-, HCC^-, and NC^-. For the hydrides, there are slight differences between the present values and those from the previous study because a slightly different scaling factor has been used for the ZPE corrections. For the three new bases, the agreement between theory and experiment is very good with errors ranging from 0.7 kcal/mol for H^- to 1.2 kcal/mol for HCC^-, well within the accuracy limits suggested by Pople for the standard G2 approach.[25,30]

2. Potential Energy Surfaces. In the study of the identity proton transfers (symmetric systems),[10] the potential energy surfaces varied from double-well potentials with a substantial central barrier to single-wells with a symmetric intermediate. A similar situation is expected in the asymmetric (nonidentity) cases, but the difference in proton affinities will have three effects: the ion−dipole complexes will have different stabilities; the transition state may occur early or late on the reaction coordinate; and the transition state barrier may be overwhelmed by the exothermicity of the proton transfer resulting in a single-well potential.

2.A. Symmetric Systems. The MP2 geometries of the complexes and transition states for the three new symmetric systems are given in Figure 2 and the energies are listed in Table 2. In each case, a double-well potential with a symmetric transition state is observed.

2.A.i. H^-/H_2. In the reaction of H^- with H_2, a very loose, linear complex is observed with an intermolecular distance of greater than 3 Å. At this level of theory, the complex is predicted to be slightly less stable than the separated reactants. Clearly the calculations are having a difficult time characterizing the interaction and the added zero-point energy of the complex is enough to make the process appear to be endothermic. Nonetheless, the H^-/H_2 complex must be very weakly bound. This

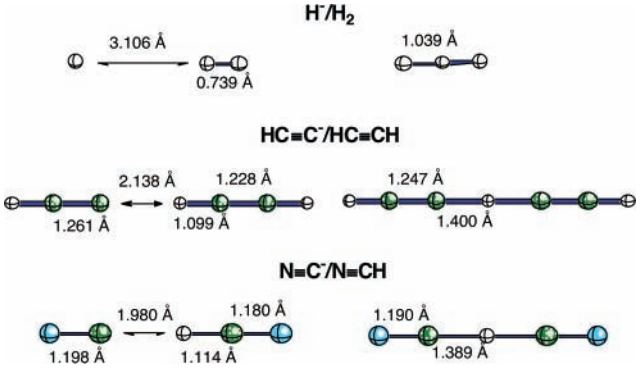

Figure 2. MP2/6-311+G(d,p) geometries of complexes and transition states in the identity reactions.

TABLE 2: G2+ Energies of Complexes and Transition States[a]

structure	relative energy	structure	relative energy
$H^- \; H_2$	0.9	$SiH_4 \; F^-$	−10.3
H−H−H⁻	11.5	SiH_3−H−F⁻	−13.8
HC≡C⁻ HC≡CH	−10.6	SiH_4F^- [b]	−39.8
HC≡C−H−C≡CH⁻	−6.8	HC≡C⁻ SiH_4	−2.6
N≡C⁻ HC≡N	−18.7	HC≡CH SiH_3^-	−9.5
N≡C−H−C≡N⁻	−15.9	HC≡CSiH_4^- [b]	−15.2
CH_3^- NH_3	−8.6	HC≡C−H−SiH_3^-	3.4
CH_4 NH_2^-	−16.6	HC≡CH F⁻	−30.5
CH_3−H−NH_2^-	−7.3	N≡C⁻ H_2S	−10.7
NH_3 OH^-	−34.5	N≡CH SH^-	−17.8
OH_2 F^-	−45.4	N≡C−H−SH^-	−12.9
SiH_3^- PH_3	−1.3	NH_2^- H_2	−1.4
SiH_4 PH_2^-	−12.6	NH_3 H^-	−8.3
SiH_3−H−PH_2^-	0.5	NH_2−H−H⁻	−2.3
PH_3 SH^-	−21.0	CH_3^- H_2	−0.5
SH_2 Cl^-	−28.9	CH_4 H^-	−14.9
SiH_3^- HF	−19.5	CH_3−H−H⁻	2.0

[a] Energies in kcal/mol. See text for details on G2+. Energies are relative to separated reactants. Reactants defined as partners in first complex listed in table. [b] Pentacoordinate silicon.

reaction should not be observable under typical gas phase conditions because the transition state is 10.8 kcal/mol less stable than the separated reactants.

2.A.ii. HCC⁻/HCCH. In the reaction of HCC− with HCCH, a linear complex with an intermolecular distance of 2.138 Å is observed. The interacting H−C bond is stretched to 1.099 Å from its normal value of 1.064 Å, indicating a reasonably strong hydrogen bonding interaction. This complex is 10.6 kcal/mol more stable than the reactants. The transition state is also linear and the bridging C−H distances are 1.400 Å. The transition state is 6.8 kcal/mol more stable than the reactants indicating a barrier of 3.8 kcal/mol with respect to the complex. The negative activation energy suggests that proton transfer should be observable under typical gas phase conditions. In previous work, Evleth[31] and Schiener[32] have found barriers of 10.9 (HF/4-31+G, no ZPE correction) and 7.6 (MP2/6-31+G**) kcal/mol, respectively, relative to the complex.

2.A.iii. NC⁻/HCN. The complex of NC⁻ with HCN is linear and is 18.7 kcal/mol more stable than the separated reactants. Several experimental values are available for the complexation energy and the NIST database reports an average value of 21 ± 1 kcal/mol.[33] The transition state is 15.9 kcal/mol more stable than the reactants and a barrier of 2.8 kcal/mol is observed relative to the complex. Very rapid proton transfer is expected in this case. Evleth[31] and Scheiner[32] also considered this system and found barriers of 7.7 and 5.3 kcal/mol, respectively.

When studying the identity proton transfer reactions of the hydrides,[10] we noted good correlations between the proton

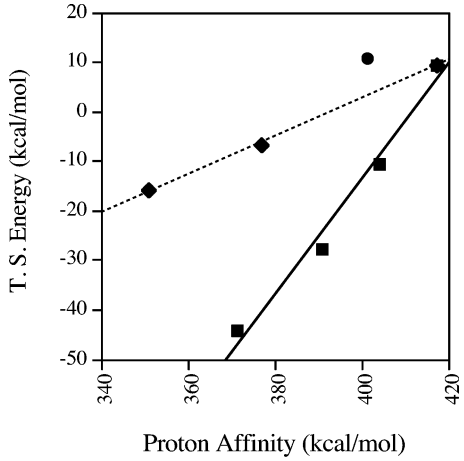

Figure 3. Plots of relative proton transfer transition state energy vs ΔH_{acid} (kcal/mol) in identity reactions. Data are from G2+ calculations. Squares with solid line represent the first-row hydrides ($CH_4 \rightarrow FH$). Diamonds represent carbon acids (HC≡N, HC≡CH, and CH_4). The circle represents H_2.

affinities and the stabilities of the transition structures; however separate correlations were found for the first and second-row systems. In Figure 3, the plot is extended to include H^-, HCC^-, and NC^-. It is clear that an excellent correlation can be found for the three carbon acids ($r^2 = 0.999$); however, this correlation is different from the one found previously for the first-row elements, and H^- fits neither one.[10] This behavior suggests that to characterize these systems, a family of correlations must be considered, one for each element. This situation has been encountered previously in condensed phase studies of proton transfer and elimination reactions.[3,34−36] The rapid increase in transition structure stability observed across the series from CH_3^- to F^- is the result of not only the decrease in proton affinity, but also the shift to more electronegative atoms (lower intrinsic barriers). Because these two factors are intimately related, it is not surprising that a smooth correlation could be observed for the series whereas a family of correlations is required to describe the behavior of derivatives of these simple bases.

2.B. Asymmetric Systems with a Barrier. In 7 of the 12 asymmetric (nonidentity) proton transfers in the present study, a transition state was identified on the electronic energy surface. The structures of the ion−dipole complexes and transition states are shown in Figure 4 and the energy data are in Table 2. These seven reactions have exothermicities that range from −15.8 kcal/mol (CH_3^-/H_2) to 0 kcal/mol (CN^-/SH_2). In two cases, NH_2^-/H_2 and NC^-/SH_2, the computed transition state energy is lower than the energy of the reactant complex. Although a barrier exists on the electronic energy surface for these reactions, differences in the thermal and ZPE corrections eliminate it. Therefore, these systems are effectively barrierless and collapse directly to the product complex. However, because a maximum exists on the electronic energy surface for these reactions, we can use that structure as a pseudotransition state for the analysis of the potential energy surface.

To judge the position of a transition state on the overall reaction coordinate, a number of approaches are possible. We will focus on two, closely related properties, the bond length to the transferring proton and the critical point density of this bond (Table 3). Although more sophisticated analyses could be devised, we will adopt a simple approach based on a comparison to the central transition states found in the parent, identity proton transfers (symmetric systems). The deviation

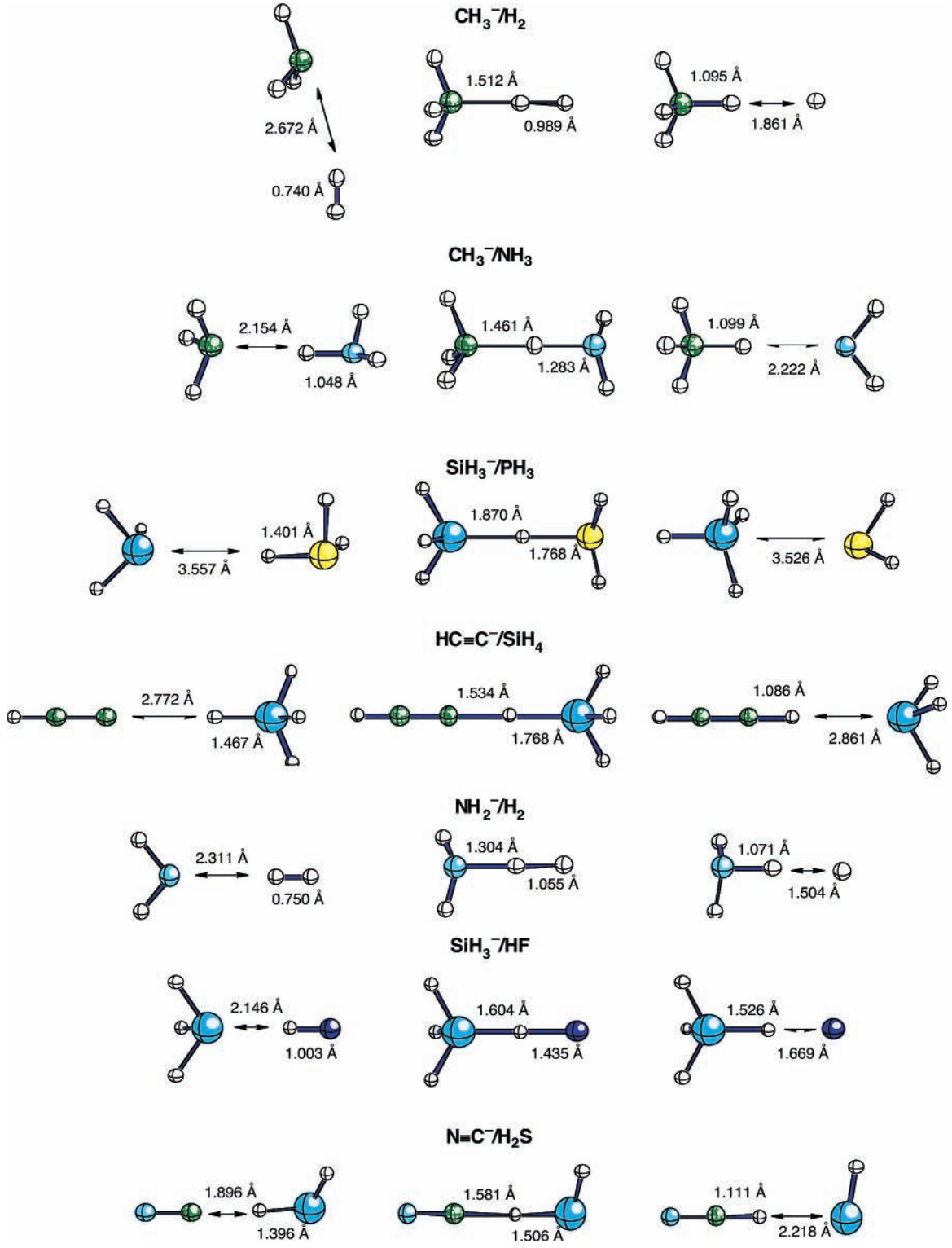

Figure 4. MP2/6-311+G(d,p) geometries of complexes and transition states in the nonidentity reactions with a barrier.

from a central transition state is taken as the difference in the transition state property (bond length or critical point density) between that found in the asymmetric and symmetric reactions. This is normalized by the overall change found for the symmetric transition state (relative to the ground state). The effect is averaged over the two bonds (the order of terms is reversed in the second bond to take into account the fact that deviations from a symmetric transition state are numerically opposite in the forming and breaking bonds). These relationships are given explicitly in eqs 1 and 2. The R_o and ρ_o values are

$$\%\ \text{deviation (bond length)} = \frac{100[[(R'_o - R')/(R'_o - R'_e)] + [(R - R_o)/(R_o - R_e)]]}{2} \quad (1)$$

$$\%\ \text{deviation (critical point density)} = \frac{100[[(\rho'_o - \rho')/(\rho'_o - \rho'_e)] + [(\rho - \rho_o)/(\rho_o - \rho_e)]]}{2} \quad (2)$$

the bond lengths and critical point densities in the symmetric

TABLE 3: Electron Density Analysis with the Bader Approach[a]

structure	ρ(X−H)	ρ(H−Y)
$HC{\equiv}C^-$ HC≡CH	0.024	0.273
HC≡C−H−C≡CH^-	0.128	0.128
N≡C^- HC≡N	0.032	0.261
N≡C−H−C≡N^-	0.130	0.130
H^- H_2	0.003	0.271
H−H−H^-	0.120	0.120
H^- NH_3	0.018	0.320
H−H−NH_2^-	0.167	0.099
H_2 NH_2^-	0.257	0.020
CH_3^- H_2	0.009	0.267
CH_3−H−H^-	0.073	0.178
CH_4 H^-	0.283	0.006
CH_3^- NH_3	0.026	0.308
CH_3−H−NH_2^-	0.117	0.163
CH_4 NH_2^-	0.279	0.018
NH_3 OH^-	0.301	0.041
OH_2 F^-	0.268	0.082
SiH_3^- PH_3	0.000	0.165
SiH_3−H−PH_2^-	0.076	0.091
SiH_4 PH_2^-	0.119	0.000
PH_3 SH^-	0.248	0.015
SH_2 Cl^-	0.209	0.029
SiH_3^- HF	0.042	0.271
SiH_4 F^-	0.123	0.048
SiH_3−H−F^-	0.115	0.084
$HC{\equiv}C^-$ SiH_4	0.008	0.126
HC≡C−H−SiH_3^-	0.096	0.092
HC≡CH SiH_3^-	0.281	0.012
HC≡CH F^-	0.221	0.084
N≡C^- H_2S	0.040	0.213
N≡C−H−SH^-	0.082	0.152
N≡CH SH^-	0.262	0.030

[a] For structure X−H−Y. ρ is critical point density in e/au^3.

TABLE 4: Analysis of Reaction Progress Using Equations 1 and 2

system	ΔH_{RXN} (kcal/mol)	ΔWD[a] (kcal/mol)	% deviation from central TS	
			bond length	critical density
CH_3^-/H_2	−15.8	−14.4	−20	−12
CH_3^-/NH_3	−12.9	−8	−8	−6
SiH_3^-/PH_3	−5.1	−11.3	2	−4
$HC{\equiv}C^-/SiH_4$	−3.7	−6.9	−33	−31
NH_2^-/H_2	−2.9	−6.9	−2	−4
SiH_3^-/HF	−2.1	9.2	96	67
$C{\equiv}N^-/SH_2$	0	−7.1	−51	−34

[a] Difference in energy between entrance and exit wells (ion/dipole complex).

transition state whereas the R and ρ values refer to the asymmetric transition state. R_e and ρ_e refer to the ground-state species (i.e., CH_4). The "primed" terms refer to the acid and the "unprimed" to the base, as defined in Table 4. In this arrangement, positive values indicate a late transition state and negative values indicate an early one. Although very simple, this analysis can give a reasonable measure of the progression along the reaction coordinate. Both approaches give qualitatively similar results.

Table 4 also lists the difference in energy between the reactant and product ion/molecule complex well depths (ΔWD). In most cases, this value is significantly different from the overall reaction energy. Of course this indicates that the ion/dipole complexation energies of the reactants and products are not the same. Most of the cases can be explained on the basis of the polarity of the neutral partner in the complex. For example, ΔWD is smaller than ΔH_{RXN} for the CH_3^-/NH_3 system because CH_4 is a poor complexing agent and therefore the product complex is less stable (relative to dissociation) than the reactant complex. A similar situation occurs (though in the reverse direction) for the NH_2^-/H_2 system. Also, there generally are large discrepancies between ΔWD and ΔH_{RXN} for reactions that involve partners with central atoms from the second and third period. This is sensible because the second period elements tend to be much better hydrogen bond donors than those from the third period so there is a significant energetic advantage when the second period partner is the neutral molecule in the complex. This is most evident in the SiH_3^-/HF system, which involves an exothermic proton transfer but has a ΔWD that is endothermic by 9.2 kcal/mol because SiH_4 makes a much weaker complex with F^- than HF does with SiH_3^-. Of course, F^- makes a very stable pentacoordinate complex with SiH_4 (Table 2), but the hydrogen bonded one (Figure 4) is rather weak. Another interesting aspect of this system is that it has a significant barrier despite the fact that the F^-/HF reaction has no barrier. Apparently, the large intrinsic barrier from the SiH_3^-/SiH_4 reaction (15 kcal/mol) pushes the system to a double-well rather than a single-well potential. All of the other reactions in this group are composed of systems where both partners have barriers on their identity reactions' electronic energy surface. Finally, the SiH_3^-/PH_3 system gives a fairly large ΔWD value because the product complex is preferentially stabilized by a Si−P rather than a hydrogen bonding interaction.

The Hammond postulate[37] provides a connection between the exothermicity of a reaction and the position of the transition state. Assuming that related processes are being compared, reactions that are more exothermic should have "earlier" transition states. One could use either ΔH_{RXN} or ΔWD as the measure of exothermicity, but the latter is more reasonable because it involves the species that flank the energy maximum on the surface. A rough correlation does exist in that the exothermic reactions (in terms of ΔWD) have early transition states (i.e., negative deviations) whereas the one reaction with a positive ΔWD, SiH_3^-/HF, has a late transition state. However, nothing close to a quantitative trend exists and attempts to find linear relationships using any of the quantities (ΔWD or ΔH_{RXN} vs either TS measure) lead to poor correlations. For example, the reactions with the earliest transition states (CN^-/SH_2 and HCC^-/SiH_4) are some of the least exothermic. Moreover, one of the most exothermic reactions (SiH_3^-/PH_3) has almost a perfectly symmetric transition state. In fact, the Si−H and P−H distances to the transferring proton are nearly the same as those in the identity transition states. Despite the lack of a quantitative correlation, two general conclusions can be drawn from the data in Table 4. First, the reactions involving central elements from the same row of the periodic table tend to have nearly symmetric transition states even when the reaction is significantly exothermic (e.g., CH_3^-/NH_3 and SiH_3^-/PH_3). The systems involving H_2 and a molecule with a second period central element also seem to fit this pattern. Second, when one partner is from the second period and the other is from the third, large deviations from a central transition state occur. This is not simply a size issue because the effect is seen in the bond length (eq 1) and critical point density (eq 2) measures of the transition state position. The divergence from central transition states in these cases can be rationalized on the basis of the relative hydrogen bonding abilities of the partners. The second period elements are significantly better hydrogen bond donors so resonance form **I** is stabilized relative to resonance form **II** in the transition state (Scheme 2). As a result, species with charge distributions such as **II** (i.e., geometries where the A_{third}−H bond is more developed than the A_{second}−H bond) are disfavored and the transition state shifts in that direction. The data in Table 4

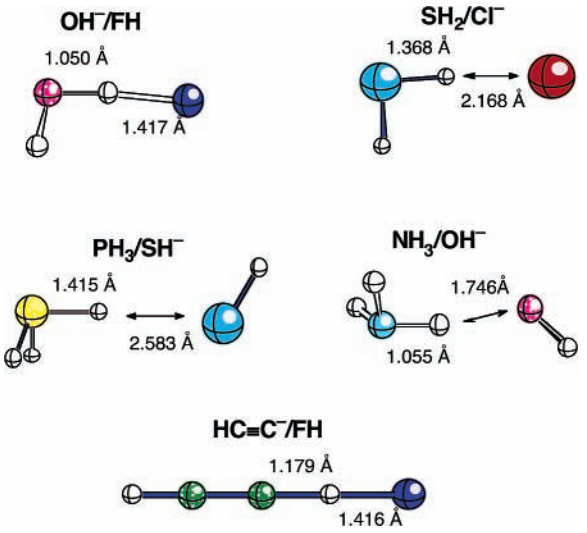

Figure 5. MP2/6-311+G(d,p) geometries of complexes in the nonidentity reactions without a barrier.

SCHEME 2

$$[A_{3rd}^{\ominus}\text{--}H\text{—}A_{2nd}] \longleftrightarrow [A_{3rd}\text{—}H\text{--}A_{2nd}^{\ominus}]$$

I **II**

confirm that when there is a large divergence from a central transition state, it is toward a more highly developed A_{third}—H bond.

2.C. Asymmetric Systems without a Barrier. In five of the reactions, there is no proton transfer barrier on the electronic potential energy surface at the MP2/6-31+G(d,p) level (Figure 5). For three of the systems (OH^-/FH, SH^-/ClH, and NH_2^-/OH_2), there are not significant barriers on the surfaces of the corresponding identity reactions, so it is not surprising that there are no barriers in the cross reactions. In the first case, the intermediate has a partially shared proton with a very strong hydrogen bond between H_2O and F^-. In the other two cases, the intermediate is the result of transferring the proton to the most basic partner and a weaker hydrogen bonding interaction is observed. In the other two systems, PH_2^-/SH_2 and HCC^-/HF, at least one of the partners has a significant barrier in its identity reaction. There is a small barrier in the PH_2^-/PH_3 identity proton transfer (1.9 kcal/mol), but apparently this is overwhelmed by the large reaction exothermicity (−17.3 kcal/mol) in the PH_2^-/SH_2 system and a single well surface corresponding to a PH_3/SH—ion/molecule complex is observed. The HCC^-/FH system is similar in that the HCC^-/HCCH identity reaction has a small barrier, but the modest exothermicity of the reaction (−5.8 kcal/mol) is enough to overcome it. However, the intermediate complex has a proton that is partially shared. The C−H bond is stretched to 1.178 Å and the H−F bond is stretched to 1.416 Å.

3. Correlations between Identity and Nonidentity Reactions. It is interesting to explore whether the potential energy surface of a nonidentity proton transfer can be estimated from the surfaces found for the corresponding identity reactions of the proton transfer partners. For the sake of simplicity, we have just averaged the properties of the identity reactions and included a term to account for the exothermicity of the process. Despite the presence of "early" and "late" transition states in the data set, we have arbitrarily included 50% of the exothermicity in the analysis. Two versions were used. The first provides the transition state energy (3a) and the second provides the barrier relative to the energy of the reactant ion/molecule complex (3b).

TABLE 5: Analyses of Barriers and TS Energies[a]

	TS		Estimates			
			TS		barrier[b]	
system	energy	barrier				
CH_3^-/H_2	2.0	2.5	2.2	(0.2)	2.9	(0.4)
CH_3^-/NH_3	−7.3	1.3	−7.1	(0.3)	1.7	(0.4)
SiH_3^-/PH_3	0.5	1.8	2.9	(2.4)	2.8	(1.0)
HC≡C⁻/SiH_4	3.4	6.0	0.8	-(2.7)	6.0	(0.0)
NH_2^-/H_2	−2.3	−0.9	−1.2	(1.1)	2.1	(3.0)
N≡C⁻/SH_2	−12.9	−2.2	−14.3	-(1.4)	−2.2	(0.0)
RMS[b]				{1.6}		{1.3}

[a] Energies in kcal/mol. See text for details of analyses. Errors are listed parenthetically next to derived values. [b] Root-mean-square deviation from G2+ calculated values for cross reaction.

These equations are related to the Marcus equation[38] but lack the higher order terms. Murdoch has referred to this part of the Marcus equation as the *additivity* terms.[39]

$$E_{TS} = E^{i}_{TS} + \Delta E/2 \tag{3a}$$

$$E_{barrier}{}^{*} = E_{barrier}{}^{i} + \Delta WD/2 \tag{3b}$$

where

$$E^{i}_{TS} = (E_{TS}(X) + E_{TS}(Y))/2$$

$$E^{i}_{barrier} = (E_{barrier}(X) + E_{barrier}(Y))/2$$

and ΔWD is the difference in ion/dipole complex well depths (product − reactant).

The results of the analyses are given in Table 5. The SiH_3^-/HF system is excluded because the HF identity reaction leads to a symmetric complex (no barrier) and therefore no intrinsic barrier or transition state energy is available. The data in Table 5 show that the estimated transition state energies (E_{TS}) and barriers ($E_{barrier}$*) are in reasonable agreement with the computed values. The greatest errors are on the order of 2−3 kcal/mol and the RMS errors are about 1.5 kcal/mol. Even the system where the transition state is more stable than the reactant complex (NC^-/H_2S) is reasonably accommodated by the analysis. Overall, it appears that this simple approach does provide an adequate description of the surfaces of the nonidentity reactions. A Marcus analysis of the data was also undertaken (data not shown), but the higher order terms did not improve the fit. Of course the Marcus relationship was developed for condensed phase reactions, and Warshel[40] has provided detailed studies on the validity Marcus-type analyses in proton transfer reactions. In the present case, it is easy to rationalize the failure of the high-order terms to improve the fit. They take into account the assumption that as the transition state shifts along the reaction coordinate (i.e., from early to late), a greater amount of the reaction exothermicity is available to stabilize the transition state. If one analyzes reactions in the exothermic direction, as has been done here, this implies that early transition states will be observed and *less* than 50% of the reaction exothermicity will be available to stabilize the transition states relative to the intrinsic barriers. As noted above, the data in Table 4 indicate that there is a poor correlation between the position of the transition state and the exothermicity of the reaction. If the transition states are not responding in the expected way to changes in exothermicity, it is no surprise that the higher-order term of the Marcus relationship would be problematic. If the amount of exothermicity released at the transition state is treated as a variable in our analysis (i.e.,

$E_{barrier}* = E^{i}_{barrier} + \Delta WD * X\%$, where X is varied), the best fit occurs, by coincidence, with a contribution of 50%. This may be a fortuitous outcome from the small data set, but it is consistent with the notion that the transition states are, to a rough approximation, central in all these systems despite the exothermicity. In earlier work involving proton bound dimers, Murdoch[39] has pointed out that the *additivity terms* of the Marcus equation (i.e., the terms in eq 3) often can provide an adequate description of the surface. It is interesting to note that the greatest deviations in the model presented in Table 5 do *not* correlate with the systems that have the greatest deviations from a central transition state. This suggests that there is only a weak coupling between the geometry of the transition and the energy available from the exothermicity at the transition state in these systems (it should be stressed that we are comparing disparate systems and a better correlation is expected in closely related systems). One might wonder about the situation in more exothermic reactions, but in those cases it is likely that the barrier will disappear altogether so no transition state will appear on the surface.

Conclusions

The data for the asymmetric proton transfers indicate that the surfaces take on a shape that is a hybridization of the shapes of the parent, symmetric proton transfers. Evidence for this comes from the fact that a simple averaging of the properties of the symmetric surfaces leads to a relatively good estimate of the properties of the asymmetric surface. In some cases, barriers disappear in the asymmetric reactions as the exothermicity of the reaction pushes the system to the most stable ion/dipole complex. It appears that the position of the transition state on the reaction coordinate does not always respond in the expected way to the exothermicity of the reaction and is more related to the properties of the proton donor/acceptor.

Acknowledgment. The support of the National Science Foundation (CHE-9974506) is gratefully acknowledged.

Supporting Information Available: Tables containing all the computed energetic data are available. This material is available free of charge via the Internet at http://pubs.acs.org.

References and Notes

(1) Ando, K.; Hynes, J. T. In *Adv. Chem. Phys.* **1999**, *110*, 381.
(2) Bagno, A.; Scorrano, G. *Acc. Chem. Res.* **2000**, *33*, 609.
(3) Bell, R. P. *The Proton in Chemistry*; Cornell University Press: Ithaca, NY, 1973.
(4) Caldin, E. F., Gold, V., Eds. *Proton-Transfer Reactions*; Chapman and Hall: London, 1975.
(5) Kirby, A. J. *Acc. Chem. Res.* **1997**, *30*, 290.
(6) Koch, H. F. *Acc. Chem. Res.* **1984**, *17*, 137.
(7) Richard, J. P.; Amyes, T. L. *Curr. Opin. Chem. Biol.* **2001**, *5*, 626.
(8) Scheiner, S. *Acc. Chem. Res.* **1994**, *27*, 402.
(9) Silverman, D. N. *Biochim. Biophys. Acta-Bioenerg.* **2000**, *1458*, 88.
(10) Gronert, S. *J. Am. Chem. Soc.* **1993**, *115*, 10258.
(11) Bernasconi, C. F.; Wenzel, P. J. *J. Am. Chem. Soc.* **2001**, *123*, 7146.
(12) Bernasconi, C. F.; Wenzel, P. J. *J. Am. Chem. Soc.* **2001**, *123*, 2430.
(13) Harris, N.; Wei, W.; Saunders: W. H.; Shaik, S. *J. Am. Chem. Soc.* **2000**, *122*, 6754.
(14) Harris, N.; Wei, W.; Saunders: W. H.; Shaik, S. *J. Phys. Org. Chem.* **1999**, *12*, 259.
(15) VanVerth, J. E.; Saunders: W. H. *J. Org. Chem.* **1997**, *62*, 5743.
(16) Bernasconi, C. F.; Wenzel, P. J.; Keeffe, J. R.; Gronert, S. *J. Am. Chem. Soc.* **1997**, *119*, 4008.
(17) Bernasconi, C. F.; Wenzel, P. J. *J. Am. Chem. Soc.* **1996**, *118*, 10494.
(18) Saunders: W. H.; Vanverth, J. E. *J. Org. Chem.* **1995**, *60*, 3452.
(19) Saunders: W. H. *J. Am. Chem. Soc.* **1994**, *116*, 5400.
(20) Bernasconi, C. F.; Wenzel, P. J. *J. Am. Chem. Soc.* **1994**, *116*, 5405.
(21) Keeffe, J. R.; Gronert, S.; Colvin, M. E.; Tran, N. L. *J. Am. Chem. Soc.*, in press.
(22) Frisch, M. J.; Trucks, G. W.; Head-Gordon, M.; Gill, P. M. W.; Wong, M. H.; Foresman, J. B.; Johnson, B. D.; Schlegel, H. B.; Robb, M. A.; Replogle, E. S.; Gomperts, R.; Anfres, J. L.; Raghavachari, K.; Binkley, J. S.; Gonzalez, C.; Martin, R. L.; Fox, D. J.; DeFrees, D. J.; Baker, J. J. P.; Pople, J. A. Gaussian92; Gaussian, Inc.: Pittsburgh, PA, 1992.
(23) Pople, J. A.; Scott, A. P.; Wong, M. W.; Radom, L. *Isr. J. Chem.* **1993**, *33*, 345.
(24) Lewis, G. N.; Randall, M.; Pitzer, K. S.; Brewer, L. *Thermodynamics*; MacGraw-Hill: New York, 1961.
(25) Curtiss, L. A.; Raghavachari, K.; Trucks, G. W.; Pople, J. A. *J. Chem. Phys.* **1991**, *94*, 7221.
(26) Bader, R. F. W. *Acc. Chem. Res.* **1985**, *18*, 9.
(27) Bachrach, S. M.; Streitwieser, A., Jr. *J. Comput. Chem.* **1989**, *10*, 514.
(28) Knop, O.; Boyd, R. J.; Choi, S. C. *J. Am. Chem. Soc.* **1988**, *110*, 7299.
(29) Bader, R. F. W.; Slee, T. S.; Cremer, D.; Kraka, E. *J. Am. Chem. Soc.* **1983**, *105*, 5061.
(30) Smith, B. J.; Radom, L. *J. Phys. Chem.* **1991**, *95*, 10549.
(31) Cao, H. Z.; Allavena, M.; Tapia, O.; Evleth, E. M. *J. Phys. Chem.* **1985**, *89*, 1581.
(32) Cybulski, S. M.; Scheiner, S. *J. Am. Chem. Soc.* **1987**, *109*, 4199.
(33) Bartmess, J. E. In *NIST Standard Reference Database Number 69*; Mallard, W. G., Linstrom, P. J., Eds.; National Institute of Standards and Technology (http://webbook.nist.gov): Gaithersburg MD, 2002.
(34) Keeffe, J. R.; Kresge, A. J. In *Investigations of Rates and Mechanisms of Reactions*; Bernasconi, C. F., Ed.; Wiley-Interscience: New York, 1986; p 747.
(35) Davies, M. H.; Robinson, B. H.; Keeffe, J. R. *Annu. Rep. A* **1973**, *70*, 123.
(36) Glad, S. S.; Jensen, F. *J. Org. Chem.* **1997**, *62*, 253.
(37) Hammond, G. S. *J. Am. Chem. Soc.* **1955**, *77*, 334.
(38) Marcus, R. A. *Annu. Rev. Phys. Chem.* **1964**, *15*, 155.
(39) Magnoli, D. E.; Murdoch, J. R. *J. Am. Chem. Soc.* **1981**, *103*, 7465.
(40) Aqvist, J.; Warshel, A. *Chem. Rev.* **1993**, *93*, 2523.